Brain Research Bulletin 109 (2014) 68–76

Brain Research Bulletin

journal homepage: www.elsevier.com/locate/brainresbull

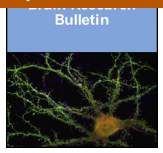

Research report

Antioxidant effects of JM-20 on rat brain mitochondria and synaptosomes: Mitoprotection against Ca^{2+}-induced mitochondrial impairment

Yanier Nuñez-Figueredo[a], Gilberto L. Pardo-Andreu[b,*], Jeney Ramírez-Sánchez[a], René Delgado-Hernández[a], Estael Ochoa-Rodríguez[c], Yamila Verdecia-Reyes[c], Zeki Naal[d], Alexandre Pastoris Muller[e], Luis Valmor Portela[e], Diogo O. Souza[f]

[a] Centro de Investigación y Desarrollo de Medicamentos, Ave 26, No. 1605 Boyeros y Puentes Grandes, CP 10600, La Habana, Cuba
[b] Centro de Estudio para las Investigaciones y Evaluaciones Biológicas, Instituto de Farmacia y Alimentos, Universidad de La Habana, Ave 23, No. 21425 e/214 y 222, La Coronela, La Lisa, CP 13600, La Habana, Cuba
[c] Laboratorio de Síntesis Orgánica de La Facultad de Química de La Universidad de La Habana, Zapata s/n entre G y Carlitos Aguirre, Vedado Plaza de la Revolución, CP 10400, La Habana, Cuba
[d] Department of Physics and Chemistry, Faculty of Pharmaceutical Sciences of Ribeirão Preto, University of São Paulo, Ave. Café s/n, 14040-903 Ribeirão Preto, SP, Brazil
[e] Departamento de Bioquímica, PPG em Bioquímica, Instituto de Ciências Básicas da Saúde, Universidade Federal do Rio Grande do Sul, Rua Ramiro Barcelos, 2600 anexo, Porto Alegre 90035-003, RS, Brazil
[f] Departamento de Bioquímica, PPG em Bioquímica, PPG em Educação em Ciência, Instituto de Ciências Básicas da Saúde, Universidade Federal do Rio Grande do Sul, Rua Ramiro Barcelos, 2600 anexo, Porto Alegre 90035-003, RS, Brazil

ARTICLE INFO

Article history:
Received 14 August 2014
Received in revised form
25 September 2014
Accepted 1 October 2014
Available online 13 October 2014

Keywords:
JM-20
Antioxidant
Mitochondria
Synaptosomes
Neuroprotector
Brain ischemia

ABSTRACT

Because mitochondrial oxidative stress and impairment are important mediators of neuronal damage in neurodegenerative diseases and in brain ischemia/reperfusion, in the present study, we evaluated the antioxidant and mitoprotective effect of a new promising neuroprotective molecule, JM-20, in mitochondria and synaptosomes isolated from rat brains. JM-20 inhibited succinate-mediated H_2O_2 generation in both mitochondria and synaptosomes incubated in depolarized (high K^+) medium at extremely low micromolar concentration and with identical IC_{50} values of 0.91 μM. JM-20 also repressed glucose-induced H_2O_2 generation stimulated by rotenone or by antimycin A in synaptosomes incubated in high sodium-polarized medium at extremely low IC_{50} values of 0.395 μM and 2.452 μM, respectively. JM-20 was unable to react directly with H_2O_2 or with superoxide anion radicals but displayed a cathodic reduction peak at −0.71 V, which is close to that of oxygen (−0.8 V), indicating high electron affinity. JM-20 also inhibited uncoupled respiration in mitochondria or synaptosomes and was a more effective inhibitor in the presence of the respiratory substrates glutamate/malate than in the presence of succinate. JM-20 also prevented Ca^{2+}-induced mitochondrial permeability transition pore opening, membrane potential dissipation and cytochrome *c* release, which are key pathogenic events during stroke. This molecule also prevented Ca^{2+} influx into synaptosomes and mitochondria; the former effect was a consequence of the latter because JM-20 inhibition followed the patterns of carbonyl cyanide *p*-trifluoromethoxyphenyl hydrazone (FCCP), which is a classic mitochondrial uncoupler. Because the mitochondrion is considered an important source and target of neuronal cell death signaling after an ischemic insult, the antioxidant and protective effects of JM-20 against the deleterious effects of Ca^{2+} observed at the mitochondrial level in this study may endow this molecule with the ability to succeed in mitochondrion-targeted strategies to combat ischemic brain damage.

1. Introduction

Oxidative stress is implicated in the pathogenesis of progressive neuron deterioration associated with excitotoxicity observed in chronic and acute brain diseases or in aging (Chen et al., 2011;

* Corresponding author. Tel.: +535 2718534.
E-mail address: gilbertopardo@infomed.sld.cu (G.L. Pardo-Andreu).

http://dx.doi.org/10.1016/j.brainresbull.2014.10.001
0361-9230/

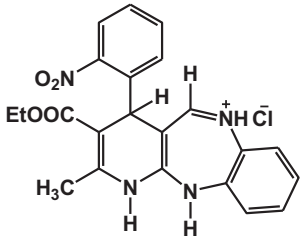

Fig. 1. Chemical structure of JM-20 (3-ethoxycarbonyl-2-methyl-4-(2-nitrophenyl)-4,11-dihydro-1*H*-pyrido[2,3-b][1,5]benzodiazepine).

Manzanero et al., 2013; Perluigi et al., 2013; Wang and Qin, 2010). Because mitochondria are the major sites for reactive oxygen species (ROS) generation in neurons (Lin and Beal, 2006), these organelles are a focus for determining new neuroprotective agents; evidence has accumulated that suggest a crucial role for mitochondrial defects in the pathogenesis of these conditions by initiating and promoting oxidative stress.

Recently, we obtained a new family of 1,5-benzodiazepines that structurally differ from the currently available 1,5-benzodiazepines due to the presence of a 1,4-dihydropyridine moiety fused to the benzodiazepine ring. JM-20 (3-ethoxycarbonyl-2-methyl-4-(2-nitrophenyl)-4,11-dihydro-1*H*-pyrido[2,3-*b*][1,5] benzodiazepine), which is a member of this compound family (Fig. 1), has an anxiolytic profile similar to that of diazepam (Figueredo et al., 2013). At a low micromolar concentration, we observed JM-20 prevents the Ca^{2+}-induced mitochondrial permeability transition, membrane potential dissipation, and pro-apoptotic protein cytochrome *c* release, and inhibits the hydrolytic activity of F_1F_0-ATP synthase in rat liver mitochondria (Nuñez-Figueredo et al., 2014a). We hypothesized that these mitoprotective effects may be involved in the neuroprotection elicited by JM-20 in several *in vitro* models relevant to cerebral ischemia (Nuñez-Figueredo et al., 2014a). We also reported an important protective effect of JM-20 against hydrogen peroxide (H_2O_2)- or glutamate-induced PC-12 cell death or KCN-mediated chemical hypoxia (Nuñez-Figueredo et al., 2014a). Because oxidative stress and mitochondrial impairment are key mediators of the ischemic process, particularly after reperfusion (Chan, 2005; Niizuma et al., 2009), we examined the antioxidant effects of JM-20 in rat brain mitochondria and in a synaptosomal preparation. To support the mitoprotective hypothesis of JM-20 neuroprotection, we also assessed its mitoprotective effect on Ca^{2+}-induced mitochondrial dysfunction using isolated mitochondria from rat brains. We observed that JM-20 acts equally as a potent antioxidant in mitochondria or in synaptosomes most likely due to its high electron-affinity at the organelle level. Our results also indicate that the mitoprotection against Ca^{2+}-mediated mitochondrial impairment may involve Ca^{2+} uptake inhibition at the mitochondrial level, which could play a role in the mechanism of action of JM-20 as a neuroprotectant.

2. Materials and methods

2.1. Compounds and reagents

All chemicals and enzymes used were of the highest grade available and were purchased from Sigma-Aldrich (St. Louis, MO, USA), unless otherwise specified. Stock solutions of JM-20 were prepared daily in dimethyl sulfoxide (DMSO) and added to the reaction media at 1/1000 (v/v) dilution. Control experiments contained DMSO at 1/1000 dilution. JM-20 was synthesized, purified and characterized as previously reported (Figueredo et al., 2013).

2.2. Isolation of synaptosomal preparation and mitochondria

The forebrains from male Wistar rats (3–4 months old) were rapidly removed and homogenized in isolation buffer containing 0.32 M sucrose, 1 mM ethylenediaminetetraacetic acid (EDTA) (K^+ salt), and 10 mM Tris–HCl (pH 7.4). The homogenate was centrifuged at 1330 × *g* for 3 min. The supernatant was carefully retained and centrifuged at 16,000 rpm (21,200 × *g*) for 10 min. The pellet was resuspended, carefully layered on the top of a discontinuous Percoll gradient and centrifuged for 5 min at 30,700 × *g* (Sims, 1990; Sims and Anderson, 2008). The synaptosomal and mitochondrial fractions were incubated in depolarized buffer (high K^+: 100 mM KCl, 75 mM mannitol, 25 mM sucrose, 5 mM phosphate, 0.05 mM EDTA, and 10 mM Tris–HCl, pH 7.4) and synaptosomal was also incubated in polarized buffer (high Na^+: 140 mM NaCl, 20 mM HEPES, 10 mM D-glucose, 1.2 mM Na_2HPO_4, 1 mM $MgCl_2$, 5 mM $NaHCO_3$, and 5 mM KCl, pH 7.4). The mitochondrial respiratory control ratio (state 3/state 4 respiratory rate ratio) was over 5, measured using 5 mM glutamate and 5 mM malate as NADH-linked substrates. Animal care followed the official governmental guidelines in compliance with the Federation of Brazilian Societies for Experimental Biology and was approved by the Ethics Committee of the Federal University of Rio Grande do Sul, Brazil.

2.3. ROS production

The mitochondrial release of H_2O_2 was assessed by the Amplex Red oxidation method. The synaptosomal or mitochondrial fractions (0.1 mg protein/ml) were incubated in the polarized or depolarized buffer supplemented with 10 μM Amplex Red and 2 units/ml of horseradish peroxidase (HRP). The fluorescence was monitored at excitation (563 nm) and emission wavelengths (587 nm) using a Spectra Max M5 microplate reader (Molecular Devices, Orleans Drive Sunnyvale, CA, USA). Catalase (EC 1.11.1.6) at 10 U/ml was used as a positive control. Each experiment was repeated 5 times with different synaptosomal or mitochondrial preparations.

2.4. Superoxide anion radical scavenging assay

Superoxide anion radical ($O_2^{\bullet-}$) generated by the xanthine/xanthine oxidase (EC 1.17.3.2) system was determined spectrophotometrically by monitoring the reduction products of nitroblue tetrazolium (NBT) (Nagai et al., 2001). The reaction mixture consisted of 3 mM xanthine, 3 mM EDTA, 15 mM NBT, and JM-20 (0.5, 1, 3, 5, 25 μM final concentrations) in 50 mM phosphate buffer (pH 7.4). After incubation at 25 °C for 2 min, the reaction was initiated by adding 0.05 U/ml xanthine oxidase and carried out at 25 °C for 10 min. The absorbance was measured at 560 nm. The reaction mixture without xanthine oxidase was used as a blank. Superoxide dismutase enzyme (SOD, EC 1.15.1.1) at 2 U/ml was used as positive control. The superoxide anion radical level was expressed as the percentage of NBT reduction *versus* control (set at 100%), which did not contain JM-20 or SOD.

The effect of JM-20 on enzyme activity was studied by estimating the uric acid formation from xanthine after 10 min incubation at 25 °C, while absorbance was measured at 295 nm. The absorbance was monitored using a Spectra Max M5 microplate reader (Molecular Devices, Orleans Drive Sunnyvale, CA, USA).

2.5. Oxygen (O_2) measurement

The O_2 consumption rates were measured polarographically using high-resolution respirometry (Oroboros Oxygraph-O2 K, Oroboros Instruments, Innsbruck, Austria). Synaptosomal or mitochondrial fractions (0.1 mg/ml) were incubated with polarized

buffer supplemented with 5 mM succinate plus 2.5 μM rotenone, or 5 mM glutamate plus 5 mM malate in the absence or presence of JM-20 for 1 min at 37 °C under continuous stirring. The respiratory protonophoric uncoupler carbonyl cyanide *p*-trifluoromethoxyphenyl hydrazone (FCCP, 1 μM) was added, and the oxygen consumption rates were registered for 10 min.

2.6. ATP assay in mitochondria

ATP was determined by the firefly luciferin–luciferase assay system (Lemasters and Hackenbrock, 1976). Mitochondria (0.1 mg/ml) were incubated in depolarized buffer energized with 5 mM glutamate plus 5 mM malate, and supplemented with 1 mM ADP. After 10 min incubation in the absence or presence of JM-20 (5 μM) or oligomycin A (1 μM), the mitochondrial suspension (0.1 mg protein/ml) was centrifuged at 9000 × *g* for 5 min at 4 °C and the pellet treated with 1 ml of ice-cold 1 M $HClO_4$. After centrifugation at 12,000 × *g* for 5 min at 4 °C, 100 μl aliquots of the supernatants were neutralized with 70 μl of 2 M KOH, suspended in 100 mM Tris–HCl, pH 7.8 (final volume, 1 ml), and centrifuged at 15,000 × *g* for 15 min. Bioluminescence was measured in the supernatant with a Sigma/Aldrich assay kit, according to the manufacturer's instructions, using an AutoLumat LB953 Luminescence photometer (Perkin-Elmer Life Sciences, Wilbad, Germany).

2.7. Electrochemical assays

Electrochemical assays were performed using a BAS CV-27 potentiostat (Bioanalytical System, Inc., West Lafayette, IN, USA) by employing conventional electrochemical cells with 3 electrodes; the data were recorded using an Omnigraphic 100 recorder (Texas Instruments, Houston, TX, USA). A 0.0314 cm^2 geometric area glassy carbon electrode, which was polished with 1 μm alumina–water suspension and rinsed thoroughly with water and acetone, was used as the working electrode. A platinum wire was used as the counter electrode, and all potentials are referenced to a sodium-saturated silver/silver chloride electrode [$Ag/AgCl/KCl_{(sat)}$] without regard for the liquid junction potential. The cyclic voltammetric studies were performed at a 100 mV/s sweep rate in 5 ml of 0.1 M phosphate buffer solution (pH 7.0), where aliquots of a 33 μM solution of JM-20 in DMSO were added. Because the cyclic voltammograms were recorded at a window potential including negative ranges, oxygen-free solution was obtained by bubbling argon through the solution. When the potential was scanned, the inert gas was kept in the solution to ensure that any oxidation reaction was not initiated by oxygen.

2.8. Determination of mitochondrial swelling, membrane potential ($\Delta\psi_m$) dissipation and cytochrome c release

Mitochondrial swelling was estimated from the decrease in the apparent absorbance at 540 nm. The mitochondrial membrane potential ($\Delta\psi_m$) was estimated spectrofluorimetrically using 10 μM Safranine *O* as a probe (Zanotti and Azzone, 1980) at the 495/586 nm excitation/emission wavelength pair. For cytochrome *c* estimation, mitochondrial suspensions were centrifuged at 12,000 × *g* in an Eppendorf centrifuge for 10 min at 4 °C, and the differential absorption spectra (reduced with dithionite/oxidized) of the supernatants were recorded in a 96-well plate (l = 1 cm). The cytochrome *c* absorption extinction coefficient ($A_{550} - A_{540}$ nm) was assumed to be 19.1 $(mM\,cm)^{-1}$ (Kruglov et al., 2008; Nuñez-Figueredo et al., 2014b). All of the experiments were performed with 1 mg/ml mitochondrial protein, incubated for 10 min in depolarized buffer (without EDTA) supplemented with 50 μM Ca^{2+} and 5 mM succinate plus 2.5 μM rotenone, in the absence (Control) or presence of JM-20 or with a mixture of ADP (250 μM) plus oligomycin A (1 μM), which is a classical combination that inhibits the mitochondrial permeability transition in rat brain mitochondria (Saito and Castilho, 2010). The absorbance or fluorescence was monitored using a Spectra Max M5 microplate reader (Molecular Devices, Orleans Drive Sunnyvale, CA, USA).

2.9. Ca^{2+} influx

Ca^{2+} influx was monitored spectrofluorimetrically using 150 nM Calcium Green-5N (Molecular Probes, OR, USA) as a probe at the 506/531 nm excitation/emission wavelength pair (Rajdev and Reynolds, 1993). The mitochondrial or synaptosomal fractions (0.1 mg protein/ml) were incubated for 1 min with JM-20 (0.5, 1, 3, 5 μM), FCCP (1 μM), Nimodipine (5 μM), or their combinations before Ca^{2+} addition (50 μM final concentration) in depolarized medium (without EDTA) energized with 5 mM succinate plus 2.5 μM rotenone. The fluorescence differences from t = 0 and t = 600 s after Ca^{2+} addition (ΔFluorescence) were recorded using a Spectra Max M5 microplate reader (Molecular Devices, Orleans Drive Sunnyvale, CA, USA).

2.10. Statistical analysis

GraphPad Prism 5.0 software (GraphPad Software Inc., USA) was used for statistical analyses. The data are expressed as the mean ± SEM. Comparisons among different groups were performed using a one-way analysis of variance (ANOVA), followed by the Newman–Keuls multiple comparison *post hoc* test. Differences were considered statistically significant at $p < 0.05$. The IC_{50} values were estimated using a non-linear regression algorithm.

3. Results

3.1. Effects of JM-20 on succinate-mediated H_2O_2 generation in rat brain synaptosomal and mitochondrial fractions under high K^+ depolarizing conditions

Fig. 2 shows that mitochondria (A) and synaptosomes (B) were responsive to succinate, as evidenced by the increase in the H_2O_2 generation rate when comparing the control (succinate) and basal rates. Additionally, JM-20 decreased H_2O_2 generation in both fractions in a concentration-dependent manner. An excess of catalase (10 U/ml) over HRP (2 U/ml) used as a positive control, almost completely reduced H_2O_2 generation, as expected. Neither succinate (5 mM) nor JM-20 (5 μM) interfered with Amplex Red florescence, after 10 min incubation in the absence of HRP (result not shown). Similar IC_{50} values were obtained for both preparations (0.91 μM), suggesting that JM-20 may act as an antioxidant at the mitochondrial level.

To improve the H_2O_2 generation capacity of the synaptosomal preparation, we used a buffer with high K^+ to depolarize the membranes and to increase the H_2O_2 production compared with the polarized buffer (Sims and Blass, 1986). This experimental strategy alters the membrane permeability during the incubation and permits the detection of classical mitochondrial responses stimulated by succinate (Sims and Blass, 1986).

3.2. Effects of JM-20 on glucose-mediated H_2O_2 generation stimulated by rotenone or by antimycin A in rat brain synaptosomes under high Na^+ polarized conditions

Considering that synaptosomal membranes depolarization by high K^+ may facilitate JM-20 entrance into synaptosomes, we also sought to determine the antioxidant effects of JM-20 under polarized (high Na^+) medium conditions. Because such conditions prevent succinate uptake by mitochondria, the rate of H_2O_2

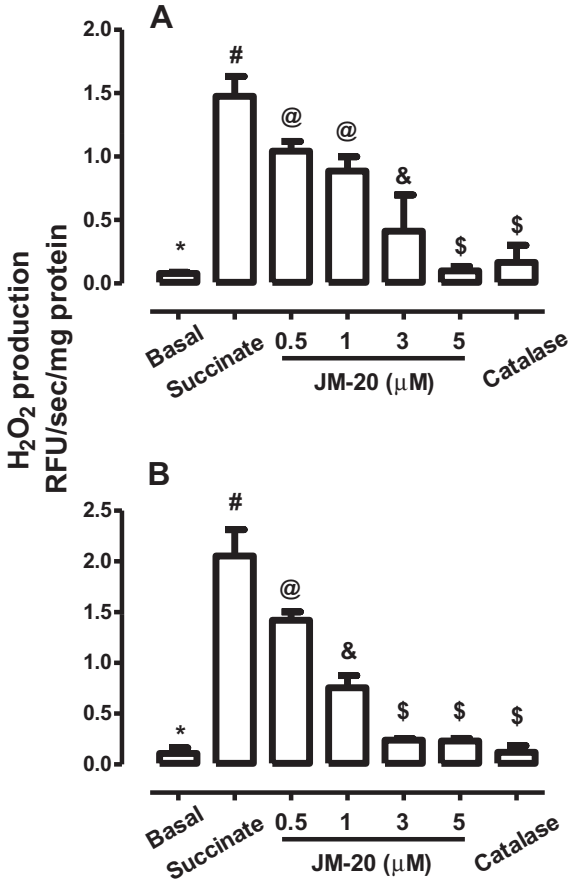

Fig. 2. JM-20 effects on succinate-induced H_2O_2 generation in rat brain mitochondrial (A) and synaptosomal (in depolarized buffer—high K^+) (B) preparations. Brain mitochondrial or synaptosomal fractions (0.1 mg proteins/ml) were incubated for 1 min with JM-20 (0, 0.5, 1, 3 and 5 μM) before succinate (5 mM final concentration) addition. Basal: no succinate and JM-20 addition. Succinate: no JM-20 addition. The reaction mixture without horse radish peroxidase (HRP) was used as a blank. The relative fluorescent units (RFU) were recorded for 10 min, and the slopes (RFU/s/mg protein) were calculated. Excess catalase (10 U/ml) over HRP was used as a positive control. The data are expressed as the mean ± S.E.M. ($n = 5$). Different symbols: $p < 0.05$ according to the ANOVA and *post hoc* Newman–Keuls tests.

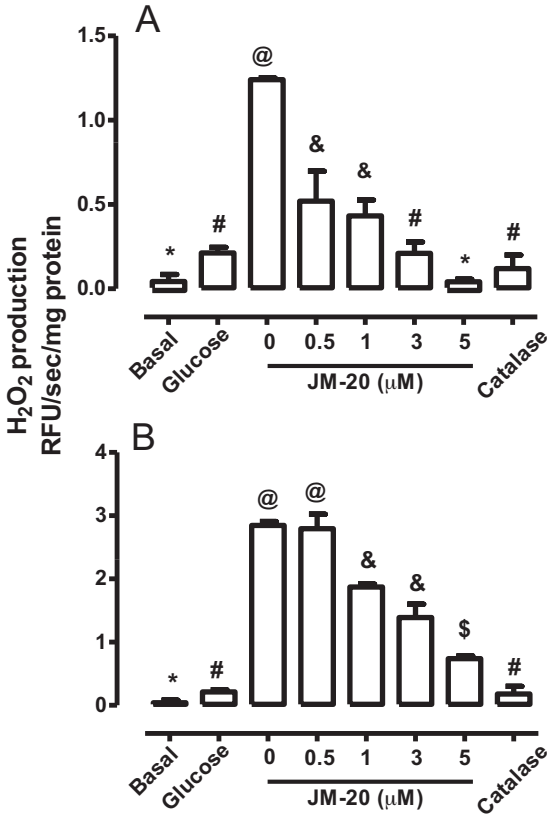

Fig. 3. JM-20 effects on glucose-induced H_2O_2 generation stimulated by (A) rotenone (Rot) or by (B) antimycin A (AA) in rat brain synaptosomes incubated in high Na^+-polarized medium. Rat brain synaptosomal fractions (0.1 mg proteins/ml) were incubated for 1 min with JM-20 (0, 0.5, 1, 3 and 5 μM) before rotenone (2.5 μM—(A)) or AA (1 μM—(B)) addition. Basal: no glucose and JM-20; glucose: with glucose and no JM-20. The reaction mixture without horse radish peroxidase was used as a blank. The relative fluorescent units (RFU) were recorded for 10 min, and the slopes (RFU/s/mg protein) were calculated. The data are expressed as the mean ± S.E.M. ($n = 5$). Different symbols: $p < 0.05$ according to the ANOVA and *post hoc* Newman–Keuls tests.

release from synaptosomes into the medium was measured after the addition of glucose, which is taken up by nerve terminals and metabolized and which serves as an energy source (Tretter et al., 2005). Fig. 3 shows that glucose slightly increased H_2O_2 production in synaptosomes; this effect was strongly potentiated by the mitochondrial complex I and III inhibitors rotenone (A) and antimycin A (B). Under both of these conditions, JM-20 also inhibited H_2O_2 generation in a concentration-dependent manner and was almost seven times more potent as an antioxidant against rotenone ($IC_{50} = 0.40$ μM) compared with antimycin A ($IC_{50} = 2.45$ μM). Glucose (10 mM), rotenone (2.5 μM), or antimycin A (1 μM) did not affect Amplex Red fluorescence after 10 min incubation in the absence of HRP (result not shown). As in Fig. 2, catalase (10 U/ml) abolished H_2O_2 generation.

3.3. Effects of JM-20 on H_2O_2 generation, HRP enzyme catalytic activity or xanthine oxidase-induced generation of superoxide anion radical in mitochondrial or synaptosomal fraction-free media

The strong antioxidant action of JM-20 against H_2O_2 generation observed under our experimental conditions could be due to (i) its direct reaction with H_2O_2; (ii) an inhibitory effect on the HRP enzyme, producing a false-positive effect; (iii) its direct reaction with superoxide anion radicals ($O_2^{\bullet -}$), preventing H_2O_2 formation; and/or (iv) its ability to prevent superoxide formation by competing with oxygen for one-electron reduction in the mitochondrial electron transport chain. We performed sets of experiments (in mitochondrial/synaptosomal fraction-free systems) aiming to understand the antioxidant mechanism of JM-20. Fig. 4 shows that JM-20 was unable to direct react with H_2O_2 (B), did not interfere with HRP catalytic function (A), and did not react with xanthine oxidase-generated superoxide anion radicals (C). This molecule did not interfere with the xanthine oxidase catalytic activity (result not shown).

3.4. Effects of JM-20 on uncoupled respiration in rat brain mitochondrial and synaptosomal fractions

Fig. 5 shows that JM-20 inhibited the O_2 consumption in isolated rat brain *mitochondrial and synaptosomal fractions*, in the presence of succinate (A) or of glutamate/malate (B). The inhibition in the presence of the NADH-linked substrates glutamate/malate was almost two times greater (approximately 30%) than that elicited in the presence of succinate, which is a $FADH_2$-related substrate (approximately 17%). Because FCCP uncouples electron transport and ATP synthesis, making oxygen consumption independent of

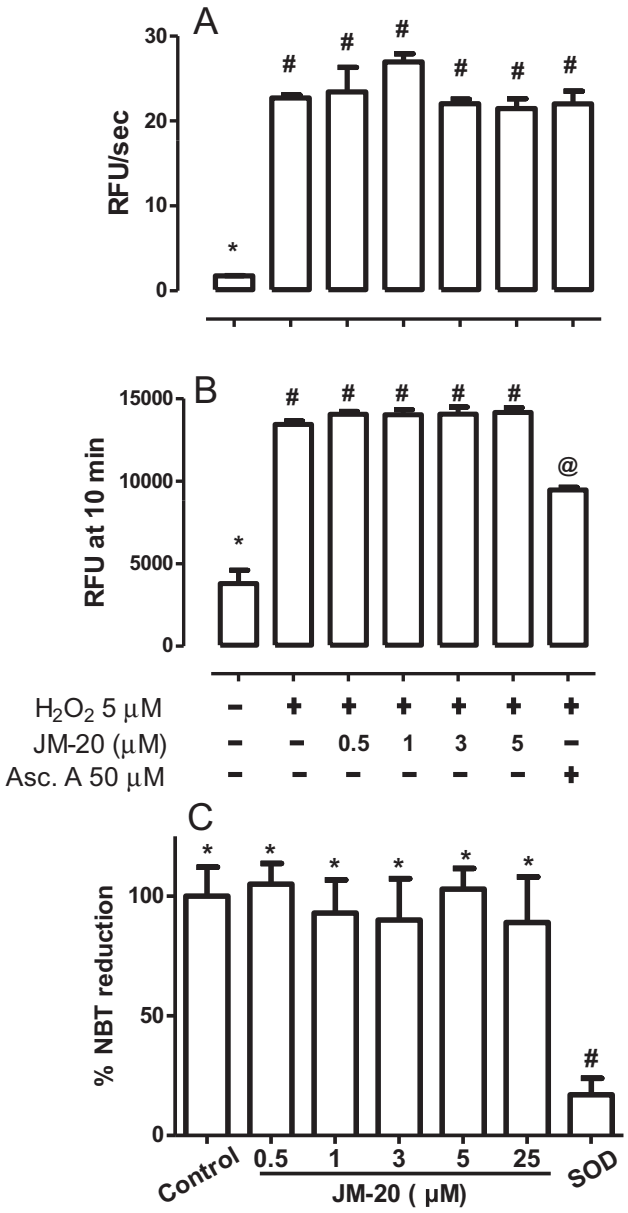

Fig. 4. JM-20 effects on HRP catalytic function (A), H_2O_2- (B) or xanthine oxidase-generated superoxide anion radicals (C) in mitochondrial/synaptosomal fraction-free medium with high K^+. The relative fluorescent units (RFU) were recorded for 10 min, and the slopes (RFU/s) were calculated to estimate the HRP enzymatic function. At 10 min of H_2O_2 incubation with JM-20, the RFU was also recorded to estimate the H_2O_2 concentration in the medium. Ascorbic acid (Asc. A, 50 µM), was used as antioxidant control. In Fig. 4C, reactions were initiated by adding xanthine oxidase (0.05 U/ml final concentration). SOD (2 U/ml) was used as positive control. The results are expressed as the percentage of NBT reduction *versus* control (set at 100%), which did not contain JM-20 or SOD. The data are expressed as the mean ± S.E.M. ($n = 5$). Different symbols: $p < 0.05$ according to the ANOVA and *post hoc* Newman–Keuls tests.

ATP generation, the observed ability of JM-20 to inhibit the respiration of FCCP-treated mitochondria indicated that this molecule did not inhibit the adenine nucleotide transporter. Since JM-20 was unable to disrupt mitochondrial membrane organization (result not shown), these results suggest that JM-20 has the ability to scavenge electrons from the mitochondrial energized membrane, diminishing the possibility of electron withdrawal and superoxide anion radical formation.

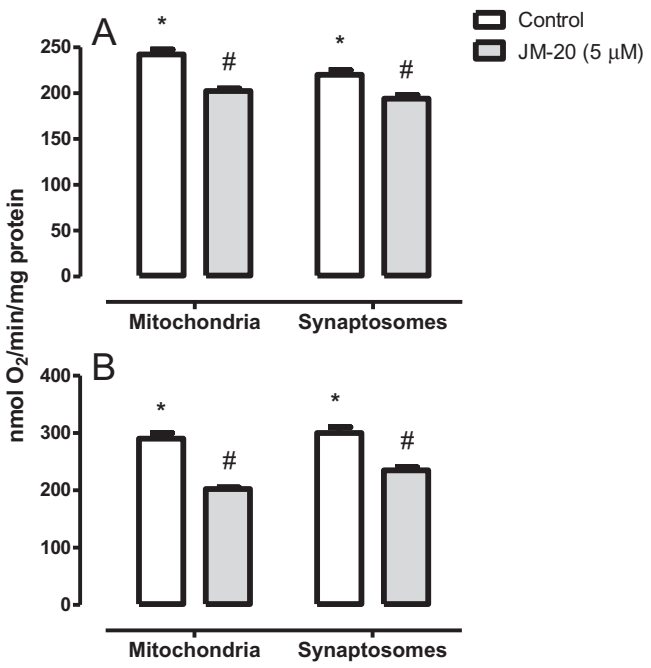

Fig. 5. JM-20 effects on uncoupled respiration in mitochondria energized with (A) succinate (5 mM) plus rotenone (2.5 µM) or with (B) glutamate (5 mM) plus malate (5 mM). Synaptosomal or mitochondrial fractions (0.1 mg/ml) were incubated with polarized buffer supplemented with the respiratory protonophoric uncoupler FCCP (1 µM) in the absence or presence of JM-20 for 10 min at 37 °C. The data are expressed as the mean ± S.E.M. of three independent experiments. Different symbols: $p < 0.05$ according to the ANOVA and *post hoc* Newman–Keuls tests.

3.5. Effects of JM-20 on mitochondrial ATP levels

To clarify whether the inhibitory effect of JM-20 on uncoupled respiration may interfere with the ATP synthesis in mitochondria, it was evaluated its effects on ATP levels. After 10-min incubation JM-20 did not affect the ATP levels of isolated rat-brain mitochondria (Fig. 6). It denotes none energetic impairment by JM-20 at comparable experimental condition to that eliciting antioxidative and Calcium protection.

3.6. Electrochemical analysis of JM-20

We also analyzed the electrochemical behavior of JM-20. A reduction peak at *ca.* −0.71 V *versus* Ag/AgCl/$NaCl_{sat}$ in the first

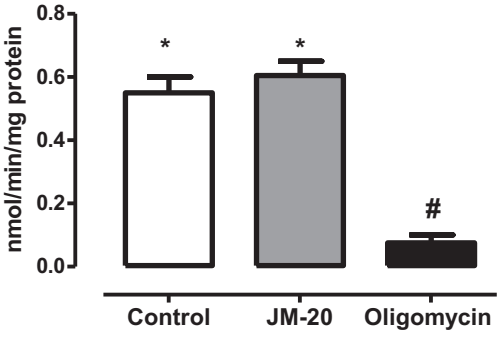

Fig. 6. Effects of JM-20 on ATP levels of isolated rat-brain mitochondria energized with 5 mM glutamate plus 5 mM malate, 10 min after incubation in depolarized medium supplemented with 1 mM ADP, as described in Materials and methods. Mitochondria (0.1 mg/ml) were incubated in the absence (Control) or presence of JM-20 (5 µM). Oligomycin A (1 µM), the classic inhibitor of the F_1F_O ATPase activity, was used as a positive control. Different symbols: $p < 0.05$ according to the ANOVA and *post hoc* Newman–Keuls tests.

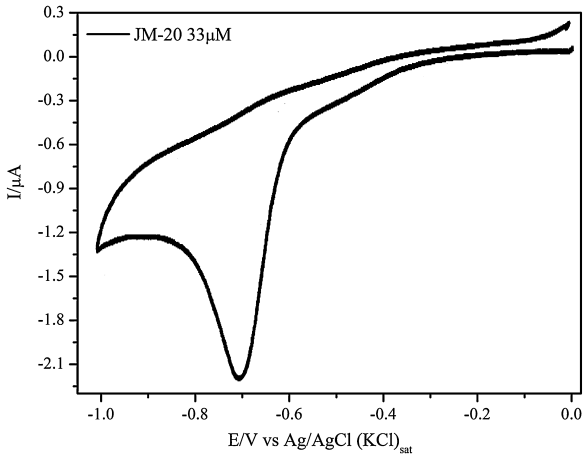

Fig. 7. Cyclic voltammograms of JM-20 (33 μM) in 0.1 M phosphate buffer solution (pH 7.0). A glassy carbon working electrode with a geometric area of 0.0314 cm^2 and a scan rate of 100 mV/s was used.

cathodic scan (Fig. 7) was observed for JM-20; we ascribed this peak to a nitro reduction mechanism (Núñez-Vergara et al., 1997). The JM-20 cathodic peak potential value is close to that of oxygen (−0.8 V), suggesting similar electron affinities and making JM-20 an oxygen competitor for electrons under low oxygen concentration. These findings may explain the antioxidant effect of JM-20 and its ability to inhibit uncoupled respiration.

3.7. *Effects of JM-20 on Ca^{2+}-mediated rat brain mitochondrial swelling, membrane potential dissipation and cytochrome c release*

A key pathogenic event during stroke is the opening of the mitochondrial permeability transition pores (mPTP) in the inner mitochondrial membrane (Hirsch et al., 1998). In the next set of experiments, we assessed the effects of JM-20 on Ca^{2+}- and Pi-induced mPTP opening, as estimated by the swelling of succinate-energized rat brain mitochondria. This classic swelling technique monitors the net influx of the osmotic support associated with a non-specific increase in membrane permeability. Fig. 8A shows that 50 μM Ca^{2+} plus 5 mM Pi induced mitochondrial swelling, as revealed by the large decrease in the turbidity of the mitochondrial suspension at 540 nm (trace a: control without JM-20). This swelling was associated with a faster mitochondrial membrane potential dissipation (Fig. 8B, Ca^{2+}). JM-20 (5 μM) almost completely inhibited both swelling and mitochondrial membrane potential dissipation (trace d, Fig. 8A and B, respectively) in a similar manner to the protection elicited by the classic mPTP inhibitor mixture ADP plus oligomycin A (trace e, Fig. 8A and B, respectively).

Cytochrome *c* release from the mitochondria plays an important role in cell death (Li et al., 1997). Because we previously demonstrated that JM-20 prevented neuronal cell death in different paradigms associated with the ischemic process (Nuñez-Figueredo et al., 2014a), next, we assessed the potential involvement of cytochrome *c* release inhibition in JM-20 effects in this study. Ca^{2+}/Pi overload induced a substantial release of cytochrome *c* from rat brain mitochondria (Fig. 8C); this effect was almost completely abolished by ADP plus oligomycin A. JM-20 (5 μM) prevented this release.

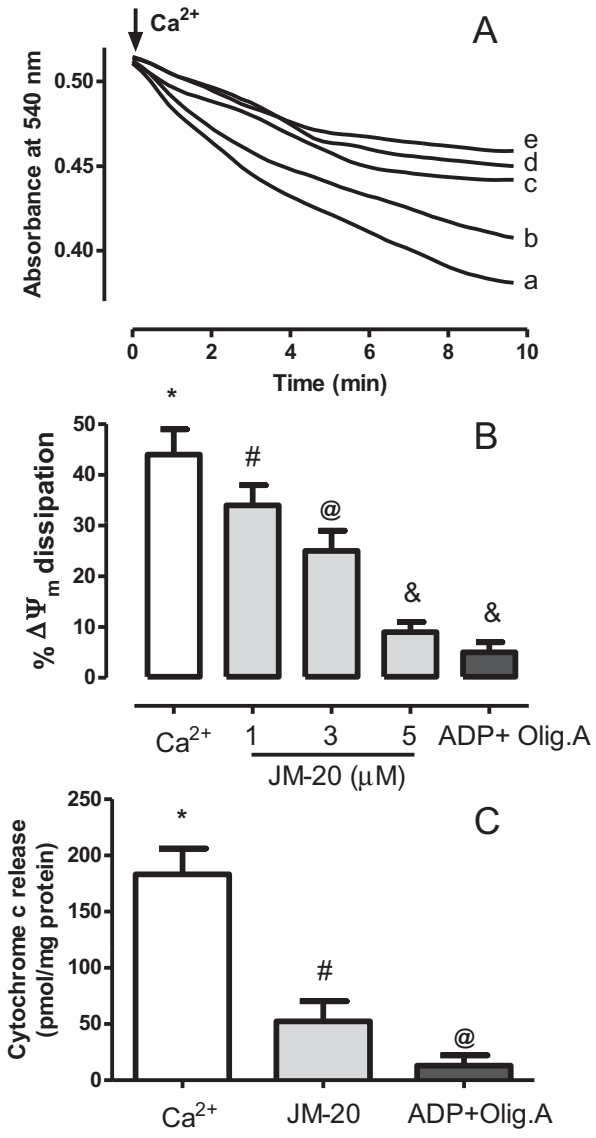

Fig. 8. Effects of JM-20 on Ca^{2+}-induced mitochondrial swelling (A), membrane potential ($\Delta\psi_m$) dissipation (B), and cytochrome *c* release (C). Rat brain mitochondria (1 mg/ml) were incubated for 10 min in depolarized medium (without EDTA) supplemented with 50 μM Ca^{2+}, 5 mM succinate and 2.5 μM rotenone in the absence (Ca^{2+}-trace a) or the presence of JM-20 (1, 3 and 5 μM-traces b, c and d, respectively) or the combination of ADP (250 μM) plus oligomycin A (Olig. A, 1 μM) (trace e). For $\Delta\psi_m$ estimation, 10 μM Safranine *O* was incorporated into the medium. In panel B, the results were expressed as *% versus* 100% $\Delta\psi_m$ dissipation induced by 1 μM carbonyl cyanide *p*-trifluoromethoxyphenyl hydrazone (FCCP, 1 μM). For cytochrome *c* release estimation, the mitochondrial suspension was sediment by high-speed centrifugation after a 10 min incubation with JM-20 (5 μM) or ADP + Olig. A. Traces in (A) are representative of five experiments conducted with different mitochondrial preparations. The data are expressed as the mean ± S.E.M. ($n = 5$). Different symbols: $p < 0.05$ according to the ANOVA and *post hoc* Newman–Keuls tests.

3.8. *Effects of JM-20 on Ca^{2+} influx into rat brain mitochondrial or synaptosomal fractions*

JM-20 inhibited Ca^{2+} influx in succinate-energized rat brain mitochondrial and synaptosomal fractions in a concentration-dependent manner (Fig. 9A). The co-incubation of FCCP with increasing concentrations of JM-20 did not increase the inhibitory potency of either compound alone (Fig. 9B), suggesting that the Ca^{2+} uptake inhibition elicited by JM-20 may be localized at the mitochondrial level. In fact, the well-known L-type Ca^{2+} channel blocker nimodipine produced approximately 50% Ca^{2+} uptake inhibition;

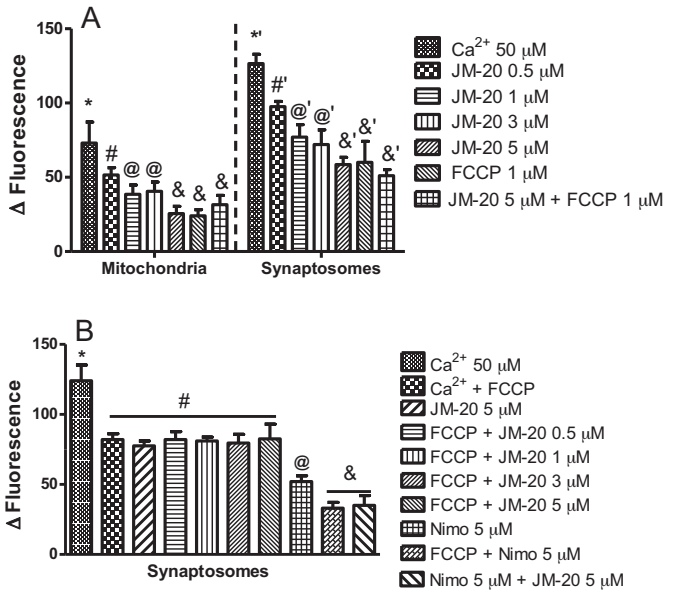

Fig. 9. JM-20 effects on Ca^{2+} influx into mitochondria or synaptosomes (A) or synaptosomes alone (B). The mitochondrial or synaptosomal fractions (0.1 mg protein/ml) were incubated for 1 min with JM-20 (0.5, 1, 3, 5 μM), FCCP (1 μM), nimodipine (Nimo, 5 μM) or their combinations in depolarizing buffer (without EDTA), before Ca^{2+} (50 μM) addition. The fluorescence differences from $t = 0$ and $t = 600$ s after Ca^{2+} addition (Δ Fluorescence) were recorded. The data are expressed as the mean ± S.E.M. ($n = 5$). Different symbols: $p < 0.05$ according to the ANOVA and *post hoc* Newman–Keuls tests.

this effect was potentiated by the mitochondrial uncoupler FCCP or by JM-20 co-incubation, thus strengthening the mitochondrial localization of JM-20 inhibitory effects on Ca^{2+} uptake.

4. Discussion

Numerous pieces of evidence show that ROS are involved in brain lesions, including those lesions due to cerebral ischemia-reperfusion (Allen and Bayraktutan, 2009; Chen et al., 2011; Manzanero et al., 2013). Mitochondria are the primary intracellular source of ROS because these organelles generate many oxidative-reduction reactions and use massive amounts of oxygen (Adam-Vizi, 2005; Lin and Beal, 2006). When anoxia is followed promptly by reperfusion, the resulting increase in oxygen supply leads to ROS overproduction (Han et al., 2001; Liu et al., 2002). In ischemic tissues, several studies have established a direct role for ROS in oxidative damage to lipids, proteins, and nucleic acids (Allen and Bayraktutan, 2009; Chen et al., 2011; Manzanero et al., 2013). Thus, mitochondria are both the initiators and the first targets of oxidative stress. Mitochondrial damage can lead to cell death, given the role of mitochondria in energy metabolism and in calcium homeostasis, as well as the ability of mitochondria to release pro-apoptotic factors, such as cytochrome *c* and apoptosis-inducing factor (AIF) (Fiskum, 2000; Fiskum et al., 1999; Lau and Tymianski, 2010; Niizuma et al., 2009). Thus, antioxidants targeting mitochondrial oxidative stress and mitoprotectors are the primary focus of neuroprotectant research. In this work, we observed that JM-20, which is a novel benzodiazepine-dihydropyridine hybrid molecule, is a strong antioxidant that acts at both synaptosomal and mitochondrial levels. Its antioxidant action was not related to its ability to scavenge superoxide anion radicals or hydrogen peroxide but to its strong electron affinity given by its low redox potential similar to that of oxygen. This electrochemical characteristic endows JM-20 with the ability to scavenge electrons from the mitochondrial electron transport chain (METC) or even to compete with oxygen for the electrons released from mitochondria, thus preventing ROS formation. We believe that the presence of a nitro group in the JM-20 dihydropyridine portion may be responsible for this antioxidant action. In this regard, the antioxidant effects of several dihydropyridine derivatives on Fe^{3+}/ascorbate-stimulated lipid peroxidation in rat brain slices has been reported (Díaz-Araya et al., 1998). Additionally, a potent reduction of alkylperoxyl and ABTS radicals by 1,4-dihydropyridines involving an electron transfer process has been documented (Yáñez et al., 2004). In fact, several 1,4-dihydropyridines inhibit oxygen consumption by *T. cruzi* Tulahueín strain epimastigotes. The drugs with higher electron-affinity produced greater inhibition than did those drugs with lower electron-affinity (Núñez-Vergara et al., 1997). These nitro-containing molecules could be reduced at the mitochondrial electron transport chain from parasites, thus inhibiting mitochondrial respiration. In the present study, we observed that JM-20 inhibited uncoupled respiration in isolated rat brain mitochondria, producing two times greater inhibition when glutamate/malate (complex I-linked substrates) were used as the energy source. This finding suggests that JM-20 reduction by the METC may involve the entire chain, particularly the upper levels of transporters where the electrochemical redox values are lower.

It is important to note that the IC_{50} value for the uncoupled respiration inhibition by JM-20 (12.31 μM) is more than 10 times higher than those for the antioxidant effects elicited by JM-20 on mitochondria or synaptosomes under depolarizing or polarizing conditions (Figs. 2 and 3). Furthermore, high thresholds of inhibition of activity of Complexes I, III and IV (more than 70%), are needed before major changes in ATP production occur in isolated brain mitochondria (Kilbride et al., 2011; Rossignol et al., 1999; Mazat et al., 2001). These circumstances make improbable that JM-20 interferes with mitochondrial respiration and ATP synthesis at antioxidative or mitoprotective concentrations as evidenced by the lack of effect of this molecule on the ATP output in tightly coupled mitochondria (Fig. 6).

Under polarized conditions (high Na^+ medium) where synaptosome membrane integrity is preserved, JM-20 also elicited strong antioxidant actions and was more potent when H_2O_2 production was stimulated by the mitochondrial complex I inhibitor rotenone. Because we observed that JM-20 did not react with H_2O_2, this result suggests that this molecule crosses synaptosomal membranes and targets mitochondria, thus preventing ROS formation. Because reactive oxygen species generated from mitochondria have been implicated in acute brain injuries, such as stroke (Manzanero et al., 2013; Niizuma et al., 2009), and because inhibiting ROS production at the source rather than scavenging the already produced oxidant agents, is already displaying positive outcomes (Hill et al., 2012; Manzanero et al., 2013), JM-20 could be a potential candidate for antioxidant therapy after ischemic brain damage.

ROS generation reduction at the mitochondrial level is not the only strategy to protect neurons after an ischemic event. Several aspects of mitochondrial function, which are not necessarily linked with ROS generation, could also be modulated to prevent mitochondrial impairment and mitochondrial-mediated apoptosis signaling initiation. In this regard, the excessive mitochondrial Ca^{2+} loading following an ischemic insult may result in mitochondrial permeability transition pore (mPTP) opening (Sullivan et al., 2005). In turn, this mPTP opening will result in a massive leak of protons and complete and immediate dissipation of the mitochondrial membrane potential, indicating a commitment to death. Cytochrome *c* release from the inter-membrane space of the mitochondria to the cytosol is one of the critical events that occur during apoptotic neuronal cell death (Fiskum, 2000; Lau and Tymianski, 2010). Because diazepam and nimodipine, both of which exhibit structural similarities to JM-20, have been reported to protect neuronal cells in different experimental models of brain ischemia *via* mitochondrial mechanisms (Sarnowska et al., 2009;

Taya et al., 2000), in the present study, we also addressed the idea that brain mitochondria are potential pharmacological targets for the neuroprotective action of JM-20. We also demonstrated the protective effect of JM-20 against Ca^{2+}-induced mPTP opening, the dissipation of the membrane potential and the inhibition of Ca^{2+}-induced cytochrome *c* release from rat brain mitochondria. JM-20 also significantly prevented mitochondrial Ca^{2+} influx, which may have been responsible for the Ca^{2+}-induced mitochondrial swelling. In this regard, abnormal Ca^{2+} accumulation by neuronal mitochondria in response to excitotoxic levels of excitatory neurotransmitters, such as glutamate, is an important mediator of mitochondrial dysfunction and of delayed cell death (Drago et al., 2011; Fiskum, 2000). Thus, JM-20-mediated protection against Ca^{2+}-induced mitochondrial impairment and its neuroprotective effects may include its ability to prevent mitochondrial Ca^{2+} influx. Notably, the inhibition of Ca^{2+} influx into synaptosomes by JM-20 followed the inhibitory patterns of the mitochondrial uncoupler FCCP and was different from that of nimodipine, which is a well-known L-type Ca^{2+} channel blocker. Indeed, the combination of FCCP with increasing concentrations of JM-20 did not induce further Ca^{2+} uptake inhibition greater than that induced by JM-20 or by FCCP alone in synaptosomes. The combination of JM-20 or FCCP plus nimodipine prompted a more than 30% increase in Ca^{2+} influx inhibition. These results suggest that the synaptosomal inhibition of Ca^{2+} uptake elicited by JM-20 is most likely related to its ability to block mitochondrial Ca^{2+} entry, similar to FCCP. This inhibition of Ca^{2+} uptake at the mitochondrial level may increase cytoplasmic Ca^{2+} concentrations in synaptosomes, thus leading to a diffusional impairment of further synaptosomal Ca^{2+} influx. Therefore, although the chemical structure of JM-20 includes a dihydropyridine moiety, JM-20 seems to be unable to block voltage-dependent Ca^{2+} channels at synaptosomal membranes under our experimental conditions. Recently, we observed that the strong neuroprotective *in vivo* effect of JM-20 against an experimental model of ischemic brain damage was related to lower Ca^{2+} accumulation into the brain mitochondria (Nuñez-Figueredo et al., 2014b). In this previous work, we raised the hypotheses that JM-20 could be inhibiting the Ca^{2+} uptake at neuronal membranes, at mitochondrial membranes, or at both levels. The present results suggest that this molecule is most likely acting at the mitochondrial level.

In conclusion, this work reveals two primary aspects of the neuroprotective mechanism of JM-20: (i) its strong antioxidant action and (ii) its protective effects against Ca^{2+}-induced impairment, which are both elicited at the mitochondrial level. The combination of two privilege structures into one molecule, a dihydropyridine moiety with a nitroaromatic group and a benzodiazepine ring supporting a net positive charge and a high level of lipophilicity, may allow the new chemical entity to cross the blood-brain barrier and cell membranes, selectively targeting mitochondria. Recently, we observed important anxiolytic and sedative effects of JM-20 on different *in vivo* experimental models with a lack of toxic effects, indicating its ability to reach the central nervous system at low doses (Figueredo et al., 2013). Because mitochondria are considered one of the important sources and targets of neuronal cell death signaling after an ischemic insult, JM-20 has the potential to succeed in mitochondrion-targeted strategies to combat ischemic brain damage.

Acknowledgments

This work was partially supported by CAPES-Brazil/MES-Cuba projects 140/11 and 092/10 and by the non-governmental organization MEDICUBA-SPAIN.

References

Adam-Vizi, V., 2005. Production of reactive oxygen species in brain mitochondria: contribution by electron transport chain and non-electron transport chain sources. Antioxid. Redox Signal. 7, 1140–1149.
Allen, C.L., Bayraktutan, U., 2009. Oxidative stress and its role in the pathogenesis of ischaemic stroke. Int. J. Stroke 4, 461–470.
Chan, P.H., 2005. Mitochondrial dysfunction and oxidative stress as determinants of cell death/survival in stroke. Ann. N.Y. Acad. Sci. 1042, 203–209.
Chen, H., Yoshioka, H., Kim, G.S., Jung, J.E., Okami, N., Sakata, H., Maier, C.M., Narasimhan, P., Goeders, C.E., Chan, P.H., 2011. Oxidative stress in ischemic brain damage: mechanisms of cell death and potential molecular targets for neuroprotection. Antioxid. Redox Signal. 14, 1505–1517.
Díaz-Araya, G., Godoy, L., Naranjo, L., Squella, J.A., Letelier, M.E., Núñez-Vergara, L.J., 1998. Antioxidant effects of 1,4-dihydropyridine and nitroso aryl derivatives on the Fe^{3+}/ascorbate-stimulated lipid peroxidation in rat brain slices. Gen. Pharmacol. 31, 385–391.
Drago, I., Pizzo, P., Pozzan, T., 2011. After half a century mitochondrial calcium in- and efflux machineries reveal themselves. EMBO J. 30, 4119–4125.
Figueredo, Y.N., Rodríguez, E.O., Reyes, Y.V., Domínguez, C.C., Parra, A.L., Sánchez, J.R., Hernández, R.D., Verdecia, M.P., Pardo Andreu, G.L., 2013. Characterization of the anxiolytic and sedative profile of JM-20, a novel hybrid molecule with putative neuroprotective activity. Neurol. Res. 35, 804–812.
Fiskum, G., 2000. Mitochondrial participation in ischemic and traumatic neural cell death. J. Neurotrauma 17, 843–855.
Fiskum, G., Murphy, A.N., Beal, M.F., 1999. Mitochondria in neurodegeneration: acute ischemia and chronic neurodegenerative diseases. J. Cereb. Blood flow Metab. 19, 351–369.
Han, D., Williams, E., Cadenas, E., 2001. Mitochondrial respiratory chain dependent generation of superoxide anion and its release into the intermembrane space. Biochem. J. 353 (Pt 2), 411–416.
Hill, M.D., Martin, R.H., Mikulis, D., Wong, J.H., Silver, F.L., Terbrugge, K.G., Milot, G., Clark, W.M., Macdonald, R.L., Kelly, M.E., et al., 2012. Safety and efficacy of NA-1 in patients with iatrogenic stroke after endovascular aneurysm repair (ENACT): a phase 2, randomised, double-blind, placebocontrolled trial. Lancet Neurol. 11, 942–950.
Hirsch, T., Susin, S.A., Marzo, I., Marchetti, P., Zamzami, N., Kroemer, G., 1998. Mitochondrial permeability transition in apoptosis and necrosis. Cell Biol. Toxicol. 14, 141–145.
Kilbride, S.M., Gluchowska, S.A., Telford, J.E., O' Sullivan, C., Davey, G.P., 2011. High-level inhibition of mitochondrial complexes III and IV is required to increase glutamate release from the nerve terminal. Mol. Neurodegen. 6, 53.
Kruglov, A.G., Subbotina, K.B., Saris, N.E.L., 2008. Redox-cycling compounds can cause de permeabilization of mitochondrial membranes by mechanisms other than ROS production. Free Rad. Biol. Med. 44, 646–656.
Lau, A., Tymianski, M., 2010. Glutamate receptors, neurotoxicity and neurodegeneration. Pflügers Arch.: Eur. J. Physiol. 460, 525–542.
Lemasters, J.J., Hackenbrock, C.R., 1976. Continuous measurement and rapid kinetics of ATP synthesis in rat liver mitochondria, mitoplasts and inner membrane vesicles determined by firefly-luciferase luminescence. Eur. J. Biochem. 67, 1–10.
Li, P., Nijhawan, D., Budihardjo, I., Srinivasula, S.M., Ahmad, M., Alnemri, E.S., Wang, X., 1997. Cytochrome *c* and dATP-dependent formation of Apaf-1/caspase-9 complex initiates an apoptotic protease cascade. Cell 91, 479–489.
Lin, M.T., Beal, M.F., 2006. Mitochondrial dysfunction and oxidative stress in neurodegenerative diseases. Nature 443, 787–795.
Liu, Y., Fiskum, G., Schubert, D., 2002. Generation of reactive oxygen species by the mitochondrial electron transport chain. J. Neurochem. 80, 780–787.
Manzanero, S., Santro, T., Arumugam, T.V., 2013. Neuronal oxidative stress in acute ischemic stroke: sources and contribution to cell injury. Neurochem. Int. 62, 712–718.
Mazat, J.P., Rossignol, R., Malgat, M., Rocher, C., Faustin, B., Letellier, T., 2001. What do mitochondrial diseases teach us about normal mitochondrial functions. . .that we already knew: threshold expression of mitochondrial defects. Biochim. Biophys. Acta 1504, 20–30.
Nagai, T., Sakai, M., Inoue, R., Inoue, H., Suzuki, N., 2001. Antioxidative activities of some commercially honeys, royal jelly, and propolis. Food Chem. 75, 237–240.
Niizuma, K., Endo, H., Chan, P.H., 2009. Oxidative stress and mitochondrial dysfunction as determinants of ischemic neuronal death and survival. J. Neurochem. 109 (Suppl 1), 133–138.
Nuñez-Figueredo, Y., Ramírez-Sánchez, J., Hansel, G., Nicoloso-Simões, E., Merino, N., Valdes, O., Delgado-Hernández, R., Lagarto-Parra, A., Ochoa-Rodríguez, E., Verdecia-Reyes, Y., Salbego, C., et al., 2014b. A novel multi-target ligand (JM-20) protects mitochondrial integrity, inhibits brain excitatory amino acids release and reduces cerebral ischemia injury in vitro and in vivo. Neuropharmacoly 85, 517–527.
Nuñez-Figueredo, Y., Ramírez-Sánchez, J., Delgado-Hernández, R., Porto-Verdecia, M., Ochoa-Rodríguez, E., Verdecia-Reyes, Y., Marin-Prida, J., González-Durruthy, M., Uyemura, S.A., Rodrigues, F.P., et al., 2014a. JM-20, a novel benzodiazepine–dihydropyridine hybrid molecule, protects mitochondria and prevents ischemic insult-mediated neural cell death in vitro. Eur. J. Pharmacol. 726, 57–65.
Núñez-Vergara, L.J., Ortiz, M.E., Bollo, S., Squella, J.A., 1997. Electrochemical generation and reactivity of free radical redox intermediates from *ortho*-and *meta*-nitro substituted 1,4-dihydropyridines. Chem.-Biol. Interact. 106, 1–14.
Perluigi, M., Swomley, A.M., Butterfield, D.A., 2013. Redox proteomics and the dynamic molecular landscape of the aging brain. Ageing Res. Rev. 13C, 75–89.

Rajdev, S., Reynolds, I.J., 1993. Calcium green-5N, a novel fluorescent probe for monitoring high intracellular free Ca^{2+} concentrations associated with glutamate excitotoxicity in cultured rat brain neurons. Neurosci. Lett. 162, 149–152.

Rossignol, R., Malgat, M., Mazat, J.P., Letellier, T., 1999. Threshold effect and tissue specificity. Implication for mitochondrial cytopathies. J. Biol. Chem. 274, 33426–33432.

Saito, A., Castilho, R.F., 2010. Inhibitory effects of adenine nucleotides on brain mitochondrial permeability transition. Neurochem. Res. 35, 1667–1674.

Sarnowska, A., Beręsewicz, M., Zabłocka, B., Domańska-Janik, K., 2009. Diazepam neuroprotection in excitotoxic and oxidative stress involves a mitochondrial mechanism additional to the GABAAR and hypothermic effects. Neurochem. Int. 55, 164–173.

Sims, N.R., 1990. Rapid isolation of metabolically active mitochondria from rat brain and subregions using Percoll density gradient centrifugation. J. Neurochem. 55, 698–707.

Sims, N.R., Anderson, M.F., 2008. Isolation of mitochondria from rat brain using Percoll density gradient centrifugation. Nat. Protoc. 3, 1228–1239.

Sims, N.R., Blass, J.P., 1986. Expression of classical mitochondrial respiratory responses in homogenates of rat forebrain. J. Neurochem. 47, 496–505.

Sullivan, P.G., Rabchevsky, A.G., Waldmeier, P.C., Springer, J.E., 2005. Mitochondrial permeability transition in CNS trauma: cause or effect of neuronal cell death? J. Neurosci. Res. 79, 231–239.

Taya, K., Watanabe, Y., Kobayashi, H., Fujiwara, M., 2000. Nimodipine improves the disruption of spatial cognition induced by cerebral ischemia. Physiol. Behav. 70, 19–25.

Tretter, L., Liktor, B., Adam-Vizi, V., 2005. Dual effect of pyruvate in isolated nerve terminals: generation of reactive oxygen species and protection of aconitase. Neurochem. Res. 30, 1331–1338.

Wang, Y., Qin, Z.H., 2010. Molecular and cellular mechanisms of excitotoxic neuronal death. Apoptosis 15, 1382–1402.

Yáñez, C., López-Alarcón, C., Camargo, C., Valenzuela, V., Squella, A., Núñez-Vergara, L.J., 2004. Structural effects on the reactivity 1,4-dihydropyridines with alkylperoxyl radicals and ABTS radical cation. Bioorg. Med. Chem. 12, 2459–2468.

Zanotti, A., Azzone, G.F., 1980. Safranine as membrane potential probe in rat liver mitochondria. Arch. Biochem. Biophys. 201, 255–265.